IEEE Photonics Journal
An IEEE Photonics Society Publication

Open Access

Theoretical Investigation of Six-Mode Multi/Demultiplexer Based on Fused-Type Multicore Fiber Coupler

Volume 8, Number 3, June 2016

Shoko Nishimoto
Takeshi Fujisawa, Member, IEEE
Yusuke Sasaki
Hitoshi Uemura
Kunimasa Saitoh, Member, IEEE

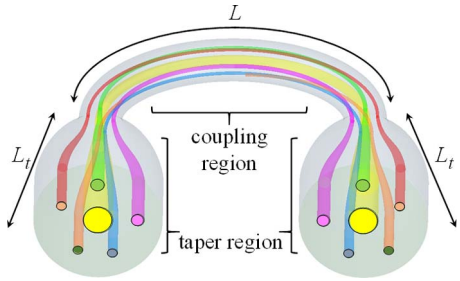

DOI: 10.1109/JPHOT.2016.2559438
1943-0655 © 2016 IEEE

Theoretical Investigation of Six-Mode Multi/Demultiplexer Based on Fused-Type Multicore Fiber Coupler

Shoko Nishimoto,[1] Takeshi Fujisawa,[1] *Member, IEEE*, Yusuke Sasaki,[2] Hitoshi Uemura,[2] and Kunimasa Saitoh,[1] *Member, IEEE*

[1]Graduate School of Information Science and Technology, Hokkaido University, Sapporo 060-0814, Japan
[2]Advanced Technology Laboratory, Fujikura Ltd., Sakura 285-8550, Japan

DOI: 10.1109/JPHOT.2016.2559438

Manuscript received March 28, 2016; revised April 20, 2016; accepted April 22, 2016. Date of publication April 27, 2016; date of current version May 10, 2016. This work was supported by the National Institute of Information and Communication Technology, Japan, under "R&B of Innovative Optical Communication Infrastructure." Corresponding author: T. Fujisawa (e-mail: fujisawa@ist.hokudai.ac.jp).

Abstract: A six-mode ($LP_{01}/LP_{11ab}/LP_{21ab}/LP_{02}$) multi/demultiplexer based on a fused-type multicore fiber coupler is proposed, and the coupling characteristics are investigated. The multi/demultiplex operation is achieved by a phase matching between the desired mode of center core and the LP_{01} mode of the outer core in the elongated region of the fused-type multicore fiber coupler. From the numerical results based on the beam propagation method, it is found that the coupling efficiencies between the LP_{01} and $LP_{11}/LP_{21}/LP_{02}$ modes are more than −0.1 dB, and the crosstalk is lower than −20 dB at the wavelength of 1550 nm.

Index Terms: Multicore fiber, mode multi/demultiplexer (MUX/DEMUX), mode-division multiplexing (MDM).

1. Introduction

Due to the rapid increase of the Internet traffic, the increased transmission capacity of the optical communication system is highly desired. However, the transmission capacity of a standard single mode fiber (SMF) is limited around 100 Tbps due to the nonlinear optical effect and the fiber fuse phenomenon [1]. To overcome the limitation, a lot of work on space division multiplexing (SDM) have been done. Among them, a mode division multiplexing (MDM) technique using few mode fibers (FMF) as a transmission medium is currently attracting a lot of attentions and being studied because of its potential for improving transmission capacity. A mode multi/demultiplexer (MUX/DEMUX) is a key component for constructing the MDM transmission system. A number of mode MUX/DEMUXs based on free-space optics [2], photonic lantern [3], planar lightwave circuit [4], and fiber coupler (FC) have been demonstrated [5]–[8]. FC-type mode MUXs are low-loss and can be directly fused to FMFs. However, in the reported structures, a precise fiber alignment method is essential for fabricating an MUX/DEMUX with sufficient performance, and the fiber for launching higher order mode is separately fused to the main fiber, and therefore, the total length of the device becomes long. To solve these issues, we have proposed and fabricated a mode MUX based on fused type multicore FC (MCFC) for three mode

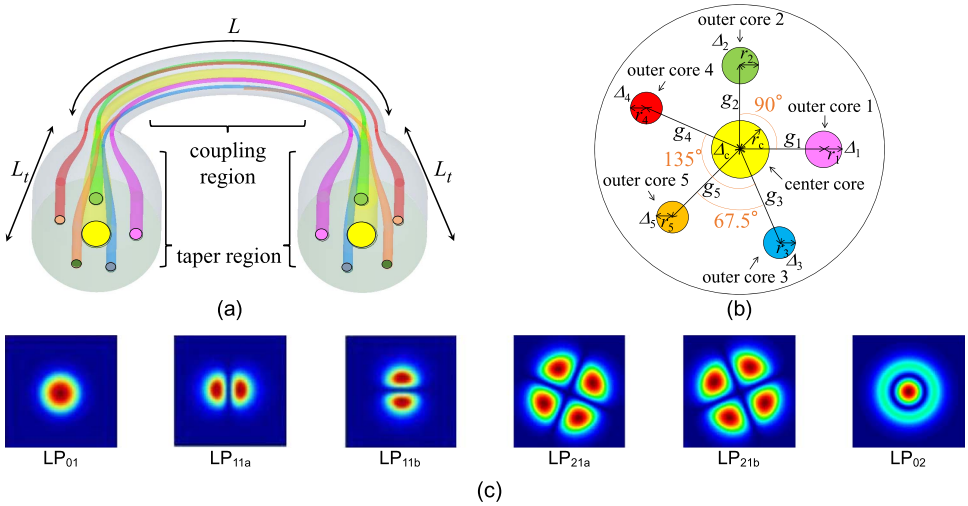

Fig. 1. (a) Schematic, (b) cross section, and (c) electric field distribution of the six-mode MUX/DEMUX based on the fused-type MCFC.

(LP_{01}/LP_{11ab}) operation, and successful three mode launch was observed [9], [10]. In our structure, since the main fiber and fibers for launching higher order mode are placed in the same fiber, the total length is shorter than those of conventional FC-type mode MUXs. In addition, the utilization of an MCFC enables precise control of the core position.

In this paper, 6 mode $(LP_{01}/LP_{11ab}/LP_{21ab}/LP_{02})$ MUX/DEMUX based on fused type MCFC is proposed, and the coupling characteristics are theoretically investigated. For launching the degenerate modes (LP_{11ab} or LP_{21ab}) separately, corresponding outer cores are placed with adequate angle with respect to the main center core. From the numerical results presented here, it is found that the coupling efficiencies for launching higher order modes are larger than −0.1 dB and the XT is lower than −20 dB for all the modes.

2. Device Structure and Operating Principle

Fig. 1 shows a (a) schematic and (b) cross-section of proposed 6 mode MUX/DEMUX based on fused type MCFC. The 6 mode MUX/DEMUX based on fused type MCFC consists of center core supporting 6 modes and five outer cores to excite higher order modes, except for the LP_{01} mode, to the center core. Each core has a step index profile. The relative refractive index difference and core radius of center core and outer core i $(= 1 \sim 5)$ are Δ_c, r_c, and Δ_i, r_i, respectively. The distance between the center core and the outer core i (core pitch) is g_i. A part of the fiber is elongated as shown in Fig. 1(a) with the length of L and we assume that the transition region is linear taper with the length of L_t. The proposed device has five regions, namely, input, input taper, coupling (elongated), output taper, and output regions. The mode launched in the outer core is designed to satisfy a phase matching condition with the center core and coupled to the center core in the elongated region. The taper ratio is t, which is defined as the ratio of the core diameter of the input (or output) and the elongated regions. In the coupling region, the effective indices of LP_{01} mode of the outer cores 1, 2, 3, 4, and 5 are matched to that of LP_{11a}, LP_{11b}, LP_{21a}, LP_{21b}, and LP_{02} modes of the center core. For LP_{11} modes, to excite degenerate modes separately, the position of the outer core 2 is rotated 90 degrees with respect to that of the outer core 1 [10]. As shown in Fig. 1(c), the LP_{11a} and LP_{11b} modes can be only launched from the outer core 1 and 2 due to the field symmetry. Similarly, outer cores 3 and 4 are placed with the 135-degree difference. Finally, the outer core 5 is placed between the core 3 and 4 since the position is the most separated from other cores.

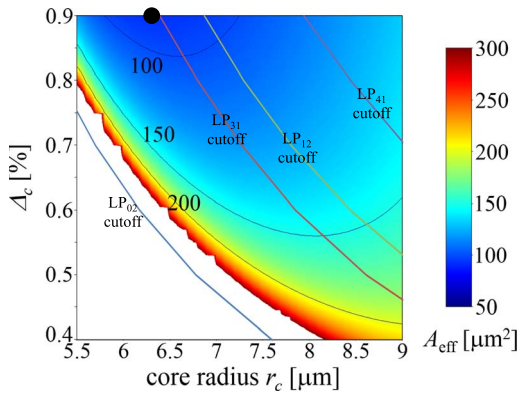

Fig. 2. A_{eff} of (color map) LP_{02} and cutoff conditions of (lines) LP_{02}, LP_{31}, LP_{12}, and LP_{41} modes as a function of r_c and Δ_c.

3. Design of Center Core

The following two characteristics are important for the design of center core of 6 mode MCFC.

1) reducing the effective area (A_{eff}) of the LP02 mode to suppress XT to other outer cores;
2) LP_{31} mode, which is the next higher mode of LP_{02}, is cut-off in the center core of the coupling region.

Characteristic 1) is important because if A_{eff} of LP_{02} mode is large, the XT to other outer cores is increased. Fig. 2 shows A_{eff} of LP_{02} (color map) and cut-off conditions of LP_{02}, LP_{31}, LP_{12}, and LP_{41} modes (lines) as a function of r_c and Δ_c. For the cut-off condition, each mode is cut-off below the line. The modal characteristics are calculated by finite-element method (FEM).

Since A_{eff} of LP_{02} mode is rapidly increased near its cut-off, r_c and Δ_c should be large (especially, Δ_c) to decrease the A_{eff}, while keeping LP_{31} mode cut-off. To meet these criteria, r_c and Δ_c in the coupling region are taken as $\Delta_c = 0.9\%$, $r_c/t = 6.3$ μm, indicated by black dot in Fig. 2. The parameters of outer cores are determined to match the effective indices of their LP_{01} mode to the desired higher order mode of the center core as shown in the next section. It should be noted that although maximum Δ_c is taken as 0.9% in this paper, the crosstalk may be suppressed for larger Δ_c, due to tighter confinement. One can choose the value depending on the fabrication technology and the target crosstalk value.

4. Coupling Properties of 6 Mode MUX/DEMUX

About the taper ratio (t), if t is large, the pitch in the coupling region is reduced, leading to the reduced coupling length and device size. However, if t is too large, the structural difference between input and coupling region is also large. Such structural difference may cause intermodal couplings between modes having similar field distribution, such as LP_{01} and LP_{02} modes for short L_t. To adiabatically taper down the structure, sufficiently long L_t is necessary, however, it makes the device size large. Here, we set $t = 1.4$, because in our previous works [9], [10], it was experimentally confirmed that LP_{01} mode in the center core is adiabatically transformed to LP_{01} in the coupling region. The next task is to determine the outer core parameters to match the effective indices of LP_{01} mode of outer cores to that of corresponding higher order modes of center core.

For $t = 1.4$, the center core radius before the elongation is $r_c = 8.82$ μm. Fig. 3 shows the outer core parameters, Δ_i, r_i, at which the phase matching condition between LP_{01} mode of the outer core and the desired higher order mode of the center core is satisfied. Solid and dashed line correspond to the fiber before and after elongation. Fig. 4 shows the coupling length in the coupling region as a function of core pitch for outer cores 1, 3, and 5. In Fig. 4, the results are plotted for two values of Δ_i for each core. For each curve, r_i is taken from Fig. 3 to satisfy the phase matching condition for corresponding Δ_i. In Figs. 3 and 4, peach, blue and orange lines

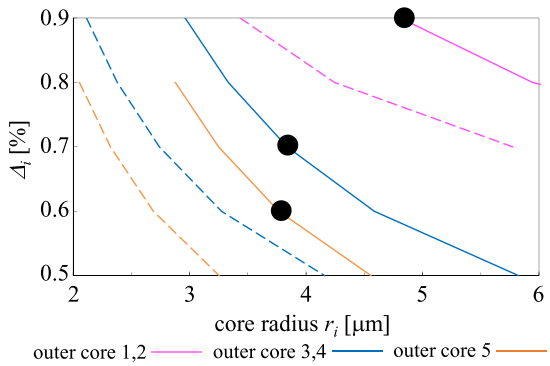

Fig. 3. Outer core parameters, i.e., Δ_i, r_i, at which the phase-matching condition between the LP_{01} mode of the outer core and the desired higher order mode of the center core is satisfied. Solid and dashed lines correspond to the fiber before and after elongation.

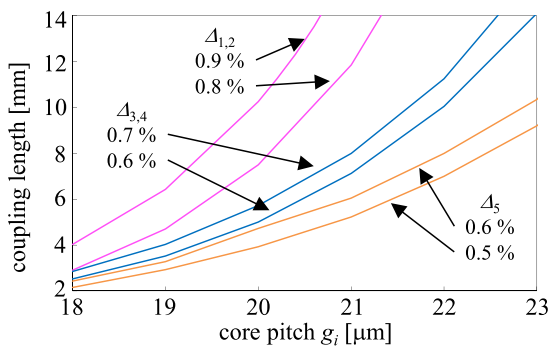

Fig. 4. Coupling length in the coupling region as a function of core pitch for outer cores 1, 3, and 5.

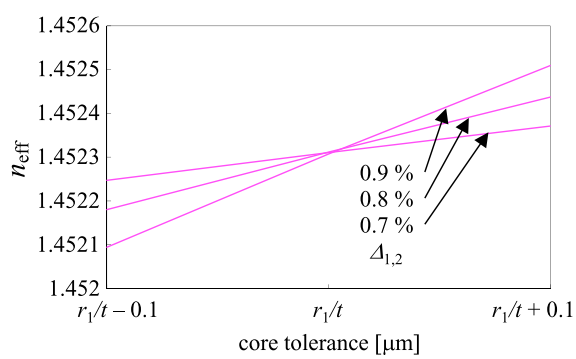

Fig. 5. n_{eff} of the outer core 1 as a function of r_1/t.

indicate the core parameters of outer cores 1, 2, outer cores 3, 4 and outer core 5, respectively. From Fig. 4, the coupling lengths between the center and outer cores can be adjusted by changing Δ_i, r_i, and g_i, and we can make three coupling lengths the same. Although one can select outer core parameters freely from the solid lines of Fig. 3, here, as a one example, parameters shown by black dots in Fig. 3 are selected for the outer cores. Namely, for outer cores 1 and 2, $\Delta_{1,2} = 0.9\%$, $r_{1,2} = 4.81$ μm, for outer cores 3 and 4, $\Delta_{3,4} = 0.7\%$, $r_{3,4} = 3.85$ μm, and for outer core 5, $\Delta_5 = 0.6\%$, $r_5 = 3.78$ μm. Fig. 5 shows effective index (n_{eff}) of the outer core 1 as a function of r_1/t. For $\Delta_1 = 0.9\%$, r_1 is 4.81 μm, for $\Delta_1 = 0.8\%$, r_1 is 5.94 μm, and for $\Delta_1 = 0.7\%$, r_1 is 8.09 μm. From Fig. 5, r_i dependence of n_{eff} is larger for large Δ. The dependence affects the core parameter tolerance of the device, as shown later in Fig. 8.

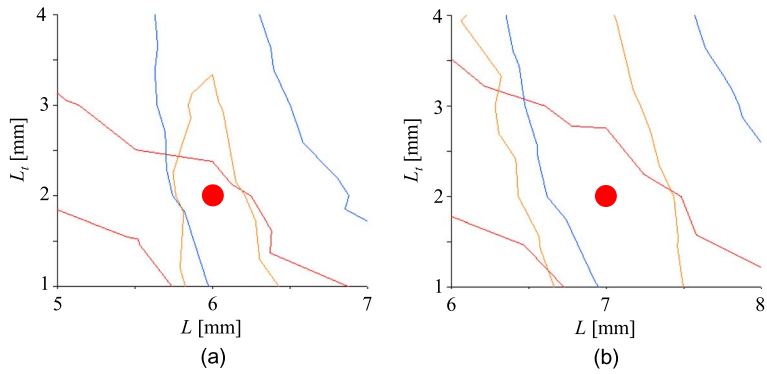

Fig. 6. L_t and L dependence of the coupling efficiencies of the desired mode in the center core at the wavelength of 1550 nm calculated by BPM for (a) the structure (1) and (b) the structure (2). The coupling efficiencies for LP_{11}, LP_{21}, and LP_{02} modes are denoted by red, blue, and orange lines, respectively.

TABLE 1

g_i used in Fig. 6(a) and (b) and of L_t and L, at which the coupling efficiencies for all the modes are large and the combination

structures	(1)	(2)
$g_{1,2}$ [μm]	19.2	19.5
$g_{3,4}$ [μm]	20.6	21.0
g_5 [μm]	21.3	21.8
L_t [mm]	2	2
L [mm]	6	7

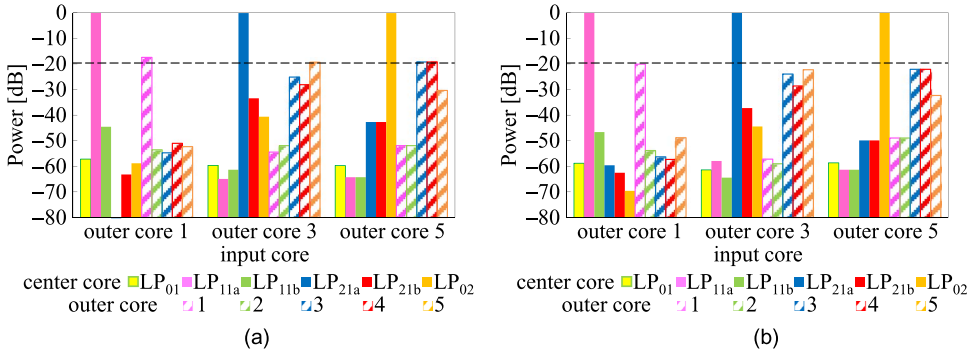

Fig. 7. Modal power variations when the light is launched from the outer cores 1, 3, and 5 for (a) the structure (1) and (b) the structure (2).

Fig. 6 shows L_t and L dependence of the coupling efficiencies of the desired mode in the center core at the wavelength of 1550 nm calculated by BPM [11], [12]. In Fig. 6(a), $g_{1,2} = 19.2$ μm, $g_{3,4} = 20.6$ μm, and $g_5 = 21.3$ μm [see structure (1)] and in (b), $g_{1,2} = 19.5$ μm, $g_{3,4} = 21.0$ μm, and $g_5 = 21.8$ μm [structure (2)]. They are summarized in Table 1. The coupling efficiencies for LP_{11}, LP_{21}, and LP_{02} modes are denoted by red, blue, and orange lines. In the region surrounded by the same color lines, the coupling efficiencies are larger than −0.2 dB. The coupling efficiency is defined as the ratio of desired mode power from the output of the center core and launched power in the corresponding outer core. For each structure, there are regions that the coupling efficiencies is larger than −0.2 dB for all the modes. The red dots in Fig. 6 show the combination of L and L_t, at which the coupling efficiencies for all the modes are large and the values are also summarized in Table 1. Fig. 7 shows the modal power variations when the light is launched from the outer cores 1, 3, and 5. Filled bars are the modal output powers from the center core, and

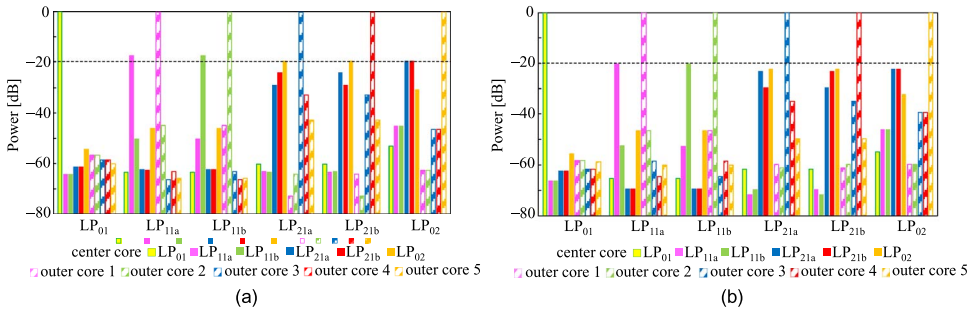

Fig. 8. Modal power variations when the light is launched from the center core for (a) the structure (1) and (b) the structure (2).

TABLE 2

Electric field distributions in the input and output sections for the structure (2) calculated by BPM

	LP_{01}	LP_{11a}	LP_{11b}	LP_{21a}	LP_{21b}	LP_{02}
input	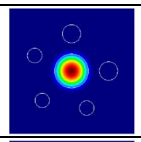	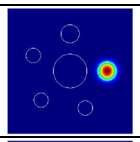	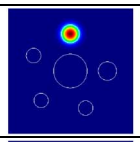	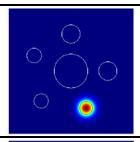	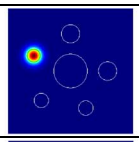	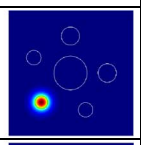
output	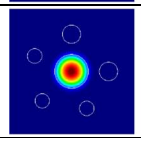	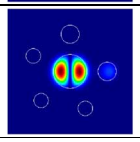	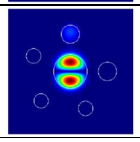	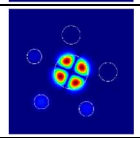	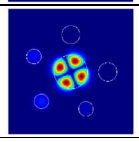	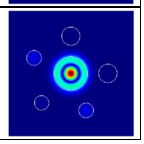

hatched bars are for the outer cores. For example, if the input core is the outer core1, the output of LP_{11a} mode in the center core (filled purple bar) should be large. Other filled bars show the XT in the center core and hatched bars show the XT in the outer cores. In this case, the purple hatched bar corresponds to the remaining power in the launched core. From the Figure, when the light is launched from the outer core 3 (LP_{21a} is launched in the center core), the XT to the outer core 5 is relatively large. However, by choosing appropriate geometrical parameters, it is possible to suppress all the XT below −20 dB with the large coupling efficiencies larger than −0.1 dB as shown in Fig. 7(b). Fig. 8(a) and (b) show the modal power variations when the light is launched from the center core (demultiplexing operation) for structures (1) and (2). In the horizontal axis, the name of mode exhibits the inputted mode in the center core. The definitions of filled and hatched bars are the same as in Fig. 7. The demultiplexing operation including a and b modes are clearly demonstrated. For structure (2), the modal XT value is lower than −20 dB for all modes as in Fig. 7(b). Table 2 shows electric field distributions in the input and output sections for the structure (2) calculated by BPM. From Table 2, coupling to the desired mode of the center core can be seen when LP_{01} mode is launched in each outer core, indicating that 6 mode including degenerated modes can be multi/demultiplexed selectively.

Fig. 9 shows wavelength and core radius dependence of the coupling efficiencies of (a) LP_{11}, (b) LP_{21}, and (c) LP_{02} modes for the structure (2). For each mode, the coupling spectra are calculated for the outer core radius of $r_i \pm 0.05$ μm. From Fig. 9, for the exact design parameters, the coupling efficiencies of $LP_{11}, LP_{21}, LP_{02}$ modes are more than −0.4 dB, −5.2 dB, and −7.6 dB in the entire C-band. The wavelength dependence is small for LP_{11} mode due to the small g_i. If the value of r_i is shifted ± 0.05 μm from the design parameters, the phase matching wavelength is shifted. The shift is largest for LP_{11} mode due to the large Δ_i. It should be noted that although for the outer core, parameters denoted by black dots in Fig. 3 are chosen for one example, one can choose different outer core parameters if they are phase matched to the

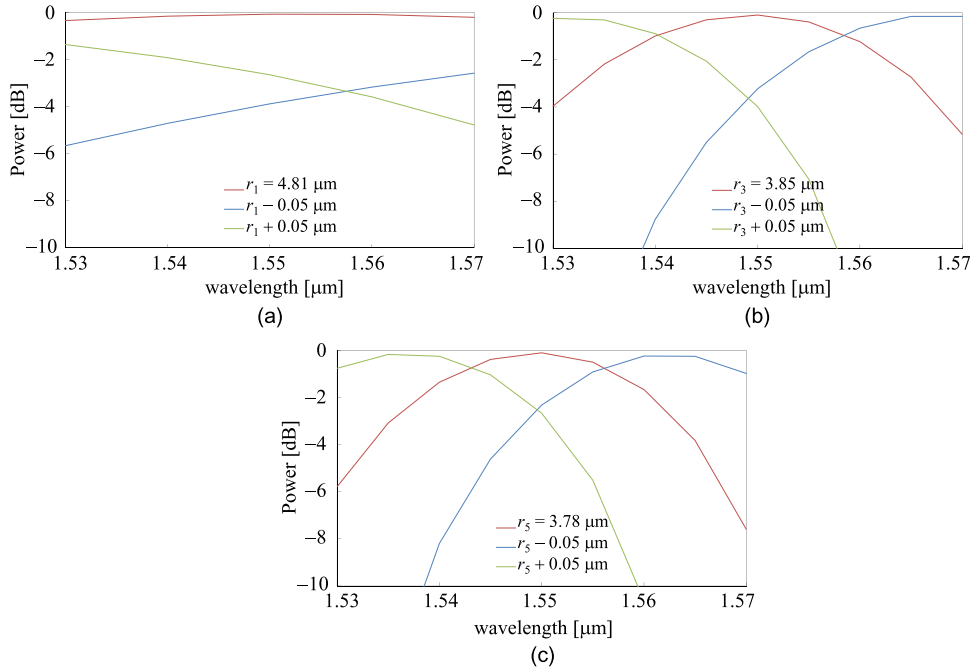

Fig. 9. Wavelength and core radius dependence of the coupling efficiencies of (a) LP_{11}, (b) LP_{21}, and (c) LP_{02} modes for the structure (2).

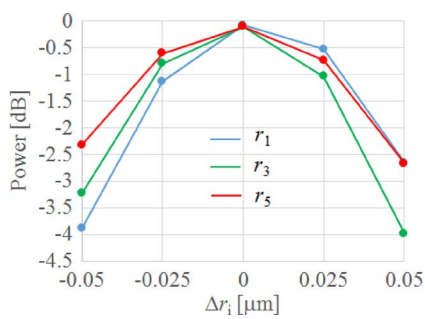

Fig. 10. Coupling efficiencies of LP_{11}, LP_{21}, and LP_{02} modes as a function of Δr_i for the structure (2) at the wavelength of 1.55 μm.

center core. Fig. 10 shows the coupling efficiencies of LP_{11}, LP_{21}, and LP_{02} modes as a function of Δr_i for the structure (2) at the wavelength of 1.55 μm. Here, Δr_i is defined as the difference with designed r_i value. The curves for r_1, r_3, and r_5 correspond to LP_{11}, LP_{21}, and LP_{02} mode, respectively. Maximum 4 dB degradation in coupling efficiency is observed for Δr_i of ± 0.05 μm.

Fig. 11 shows the wavelength dependence of the crosstalk to outer cores when the light is launched from core 1 for different values of r_1. For ideal value of r_1, the crosstalk in core 1 (remaining power) is below 10 dB, and the crosstalk to other cores are below −45 dB in the entire C-band. For core radius variations with ± 0.05 μm, the remaining power in core 1 is sharply increased due to the phase mismatch with the center core, while the crosstalk to cores 2 to 5 are still below −45 dB in the entire C-band.

5. Conclusion

We proposed 6 mode MUX/DEMUX based on fused type MCFC. By placing the outer core appropriately, 6 modes, including degenerate modes, can be launched separately. The coupling characteristics were thoroughly investigated based on FEM and BPM. From the numerical

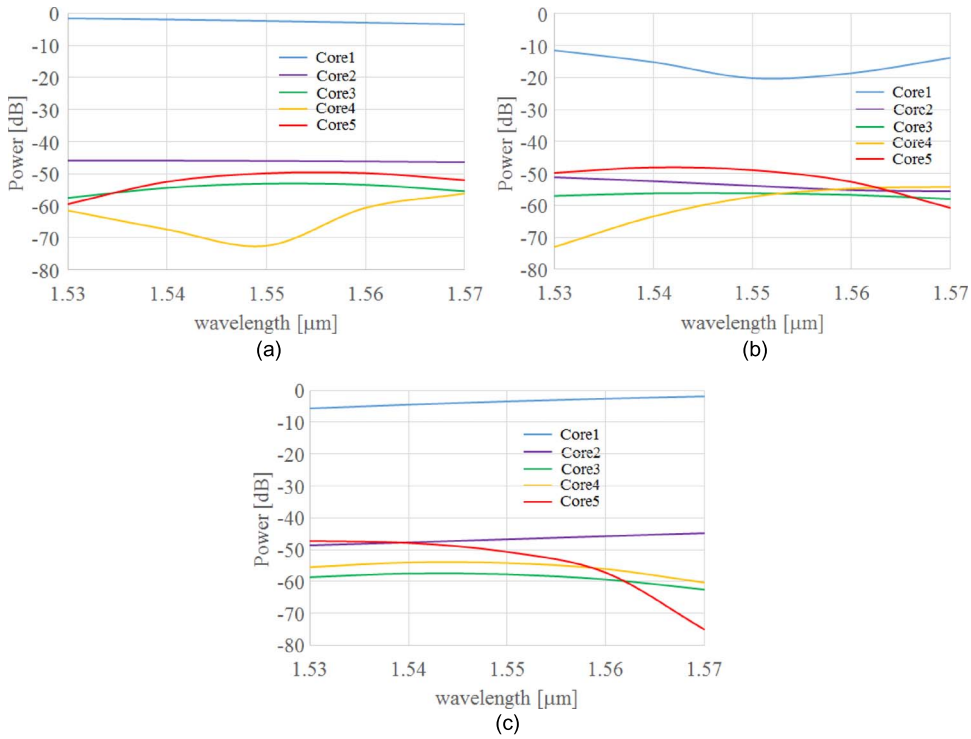

Fig. 11. Wavelength dependence of the crosstalk to outer cores when the light is launched from core 1 for (a) $r_1 - 0.05$ μm, (b) r_1, and (c) $r_1 + 0.05$ μm.

results, it was found that large coupling efficiency (> −0.1 dB) with lower XT (< −20 dB) design is possible. The proposed MCFC is a promising candidate for low-loss and easy-connection mode MUX/DEMUX.

References

[1] T. Morioka, "New generation optical infrastructure technologies: 'EXAT initiative' towards 2020 and beyond," in *Proc. IEEE OECC*, 2009, pp. 1–2.
[2] P. Genevaux *et al.,* "6-mode spatial multiplexer with low loss and high selectivity for transmission over few mode fiber," in *Proc. IEEE OFC*, 2015, pp. 1–3.
[3] B. Huang *et al.,* "All-fiber mode-group-selective photonic lantern using graded-index multimode fibers," *Opt. Exp.*, vol. 23, no. 1, pp. 224–234, Jan. 2015.
[4] N. Hanzawa *et al.,* "Demonstration of PLC-based six-mode multiplexer for mode division multiplexing transmission," in *Proc. IEEE ECOC*, 2015, pp. 1–3.
[5] S. H. Chang *et al.,* "Mode division multiplexed optical transmission enabled by all-fiber mode multiplexer," *Opt. Exp.*, vol. 22, no. 12, pp. 14229–14236, Jun. 2014.
[6] R. Ismaeel, T. Lee, B. Oduro, Y. Jung, and G. Brambilla, "All-fiber fused directional coupler for highly efficient spatial mode conversion," *Opt. Exp.*, vol. 22, no. 10, pp. 11610–11619, May 2014.
[7] K. J. Park, K. Y. Song, Y. K. Kim, and B. Y. Kim, "All-fiber mode division multiplexer optimized for C-band," in *Proc. IEEE OFC*, 2014, pp. 1–3.
[8] C. P. Tsekrekos and D. Syvridis, "Symmetric few-mode fiber couplers as the key component for broadband mode multiplexing," *J. Lightw. Technol.*, vol. 32, no. 14, pp. 2461–2467, Jul. 2014.
[9] H. Uemura *et al.,* "Mode multiplexer/demultiplexer based on a partially elongated multi-core fiber," in *Proc. IEEE OFC*, 2014, pp. 1–3.
[10] K. Takenaga *et al.,* "Multicore fibre-based mode multiplexer/demultiplexer for three-mode operation of LP01, LP11a, and LP11b," in *Proc. IEEE ECOC*, 2014, pp. 1–3.
[11] K. Saitoh and M. Koshiba, "Approximate scalar finite-element beam-propagation method with perfectly matched layers for anisotropic optical waveguides," *J. Lightw. Technol.*, vol. 19, no. 5, pp. 786–792, May 2001.
[12] T. Fujisawa and M. Koshiba, "Full-vector finite-element beam propagation method for three-dimensional nonlinear optical waveguides," *J. Lightw. Technol.*, vol. 20, no. 10, pp. 1876–1884, Oct. 2002.